Artificial Neural Networks for Fast and Accurate EM-CAD of Microwave Circuits

Gregory L. Creech, *Member, IEEE,* Bradley J. Paul, Christopher D. Lesniak, Thomas J. Jenkins, *Member, IEEE,* and Mark C. Calcatera, *Member, IEEE*

***Abstract*— A novel approach for achieving fast and accurate computer-aided design (CAD) of microwave circuits is described. The proposed approach enhances the ability to utilize electromagnetic (EM) analysis techniques in an interactive CAD environment through the application of neurocomputing technology. Specifically, a multilayer perceptron neural network (MLPNN) is implemented to model monolithic microwave integrated circuit (MMIC) passive elements using the element's physical parameters. The strength of this approach is that only a minimum number of EM simulations of these passive elements are required to capture critical input–output relationships. The technique used to describe the data set required for model development is based on a statistical design of experiment (DoE) approach. Data generated from EM simulations are used to train the MLPNN which, once trained, is capable of modeling passive elements not included in the training set. The results presented indicate that the MLPNN can predict the s-parameters of these passive elements to nearly the same degree of accuracy as that afforded by EM simulation. The correlations between the MLPNN-computed and EM-simulated results are greater than 0.98 for each modeled parameter.**

***Index Terms*— CAD, electromagnetic, microwave, neural networks.**

I. Introduction

FOR MMIC DESIGN, the effectiveness of modern computer-aided design (CAD) methods relies on accurate models of active and passive circuit elements. As circuit densities and operating frequencies increase, the accuracy of conventional modeling techniques become questionable. Typical circuit simulator supplied passive element models do not accurately account for the parasitic and coupling effects which occur at microwave/millimeter-wave frequencies [1]. To remedy this situation, libraries of passive components have been developed by actually fabricating, testing, and storing the results of hundreds of elements in a table [2]. This approach is problematic since the libraries are process dependent, costly to create, and limits the designer to a discrete set of components. Table look-up techniques, while very fast, suffer from the large memory requirements associated with the size of the table.

More recently, electromagnetic (EM) analysis tools have become commercially available which accurately model passive structures into the millimeter-wave frequency range [3]. EM simulation effectively models passive element dispersion and mutual coupling effects ignored by traditional circuit simulation tools. However, EM simulation methods, such as those in [4], take tremendous computational efforts and are not practical for interactive CAD.

In this paper, a methodology is described in which a multilayer perceptron neural network (MLPNN) is implemented to model monolithic integrated circuit (IC) passive elements to nearly the same degree of accuracy as that afforded by EM simulation. Experiments are discussed in which the s-parameters of microstrip square spiral inductors are modeled. Inputs to the neural network model are the physical dimensions of the inductor and the desired frequency. The outputs are the s-parameters for that inductor at the respective frequency points. A statistical design of experiment (DoE) approach was taken when generating the training and test data to ensure adequate parameter coverage. Once trained, the computation time of the modeled parameters is negligible, which makes the MLPNN models suitable for interactive CAD applications. Furthermore, the MLPNN's ability to generalize may eliminate the need to always perform such time-consuming EM simulations.

To demonstrate the application of this technique, three experiments were conducted. In each experiment, an MLPNN was trained to predict the s-parameters of MMIC square spiral inductors in 1-GHz steps. A C-band (4–8 GHz), X-band (8–12 GHz), and C–X band (4–12 GHz) MLPNN inductor model was developed. In each experiment, the MLPNN model's performance remained nearly constant. Therefore, only the results from the most complex experiment, the C–X-band model, are provided. The s-parameters used to train and test the MLPNN were obtained from full-wave EM simulations. Also, the MLPNN's ability to generalize the s-parameters of inductors outside the training set of each example is demonstrated.

In Section II, the MLPNN architecture and the MLPNN modeling methodology is presented. Section III describes the DoE approach for creating the comprehensive set of training data for the MLPNN inductor models described in Section IV. Finally, Section V presents the modeling results and Section VI discusses some observations and issues associated with the implementation of the MLPNN models.

II. Multilayer Perceptron Neural Network

Neurocomputing technologies have emerged as powerful modeling techniques. The class of neural network and/or architecture selected for a particular model implementation is dependent on the problem to be solved. The neural network architecture used in this modeling effort is the MLPNN.

Manuscript received September 4, 1996; revised November 21, 1996.

The authors are with the Electron Devices Division, Avionics Directorate, Wright Laboratory, Wright-Patterson AFB, Dayton, OH 45433-7319 USA.

Publisher Item Identifier S 0018-9480(97)03108-6.

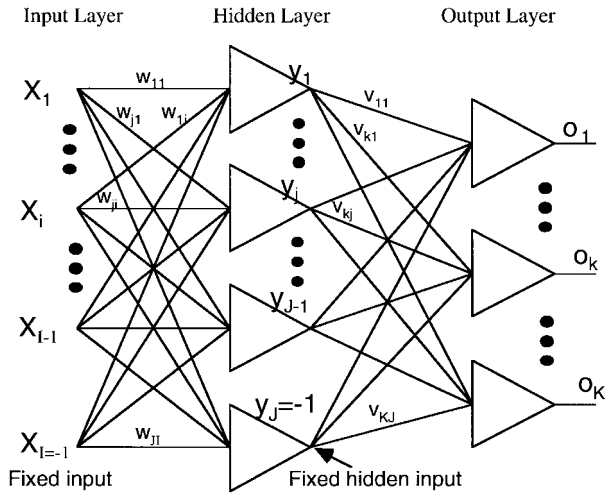

Fig. 1. MLPNN feedforward architecture.

The MLPNN is trained in the supervised mode using the error back-propagation (BP) algorithm. These networks can, in theory, perform any complex nonlinear mappings [5], [6]. Relationships are mapped between input and output data through an adaptive weight connection matrix [7].

Feedforward neural networks have recently been applied in such areas as microwave circuit analysis and optimization [8], microstrip circuit design [9], and device characterization for very large scale integration (VLSI) simulation [10]. More recently, the MLPNN has demonstrated, with good accuracy, the ability to model GaAs MESFET process and device characteristics in the forward direction [11] and to predict MESFET parametric yield [12].

A. Architecture and MLPNN Considerations

A comprehensive presentation of the MLPNN is presented in [13]; however, for convenience a brief discussion is provided here. The MLPNN has a multilayer feedforward architecture, as shown in Fig. 1. It is composed of layers of computing nodes termed neurons. Each neuron forms a weighted sum of its inputs which is passed through a nonlinear activation function. The nonlinear activation function used in this research is the sigmoidal function, $f(\text{net})$, and is expressed as

$$f(\text{net}) = \frac{2}{1 + e^{(-\lambda \text{net})}} - 1 \tag{1}$$

where net, is the weighted sum of the inputs and λ determines the gain of the neuron.

The input vector feeds each of the hidden layer neurons and the hidden layer response $\mathbf{y}$ is computed. The hidden layer response is then fedforward to the output layer and the output $\mathbf{o}$ is computed. In matrix notation this is expressed as

$$\mathbf{o} = \Gamma[\mathbf{v}\Gamma[\mathbf{wx}]] \tag{2}$$

where Γ, $\mathbf{x}$, $\mathbf{w}$, and $\mathbf{v}$, are the nonlinear operator $f(net)$, the input vector, the matrix of weights between the input and hidden layer, and the matrix of weights between the hidden and output layers, respectively.

B. MLPNN Model Development

1) Data Preprocessing and Training: Model development starts with selecting, analyzing, and manipulating data. The data to be mapped must be arranged into input–output pairs. Also, the modeler must consider how to divide the data into separate training and test files. The input–output pairs in the training file are used for model development while the test file is used for model validation. In this research a fractional–factorial experimental design was used to generate the test and training data files. This approach is described in detail in Section III. The data in these files are normalized by scaling them between the range of -1 to 1. This helps prevent the activation values from becoming too large and the occurrence of neuron saturation during training.

The MLPNN models are developed using supervised training. The network learns the mappings directly from instances of the input–output pairs in the training file. Training is facilitated through the application of the BP training algorithm. The BP algorithm, a gradient search technique, calculates the weight adjustment using the generalized delta learning rule. For each pair of input–output vectors in the training set, a weight adjustment is calculated to reduce the error between the MLPNN computed and the desired response. A thorough discussion of the generalized delta learning rule and the error BP training algorithm is presented in [13].

2) Evaluation/Validation: The goal, during training, is for the network to learn the complex mapping present in the training data and to produce accurate predictions or generalizations. Generalization is the network's ability to interpolate or extrapolate with data not included in the training set.

In this work, the testing technique used to evaluate the MLPNN's generalization capability is called cross validation [5]. Cross validation is a statistical technique in which the training sample and a validation sample are selected from the same population. The MLPNN is trained using the training sample. When the training error stops decreasing by an appreciable amount, the training is halted. The generalization capability of the network is then tested using the validation sample.

During training, the algorithm cycles through the data repeatedly, changing the weight values to improve performance. After each pass through the training data, network performance is measured by calculating the rms normalized error given by

$$E_{\text{rms}} = \frac{1}{PK} \sqrt{\sum_{p=1}^{P} \sum_{k=1}^{K} (d_{pk} - o_{pk})^2} \tag{3}$$

where P is the number of patterns in the training set and K is the number of outputs.

Training is halted when the performance stops improving. The network is then tested using the validation sample. The network's generalization is measured by computing the cumulative root mean square error (rmse) as

$$\text{rmse} = \frac{1}{P} \sqrt{\sum_{p=1}^{P} (d_p - o_p)^2} \tag{4}$$

for each individual modeled output usually denoting a single function of many variables.

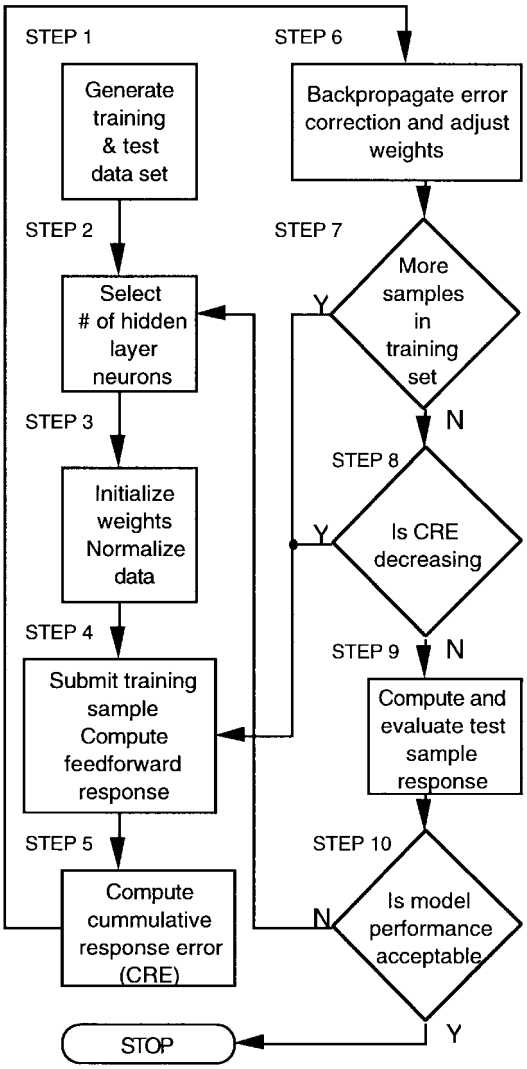

Fig. 2. Flow diagram of the MLPNN model development process.

The number of neurons in the hidden layer are then changed, and the entire process is repeated. The MLPNN exhibiting the lowest rmse is selected as the final model. The weights are then stored in a file for future implementations.

Fig. 2 is a flow diagram of the MLPNN model development process. The diagram summarizes the previous section, outlining the major steps required when creating an MLPNN model. The flow diagram is presented in the form of an algorithm; however, human interaction is necessary at several steps.

III. DoE and EM Simulations

In this research, a fractional–factorial experimental design was used to generate the test and training data. The technique is analogous to traditional DoE's [14]. Significant factors were selected and varied according to predetermined levels. However, unlike traditional DoE, the results of the experiments were not modeled using regression. Instead, the results were modeled using an MLPNN. A full factorial design was not used since some factor levels would have produced nonorthogonal factors or would not have been physically realizable.

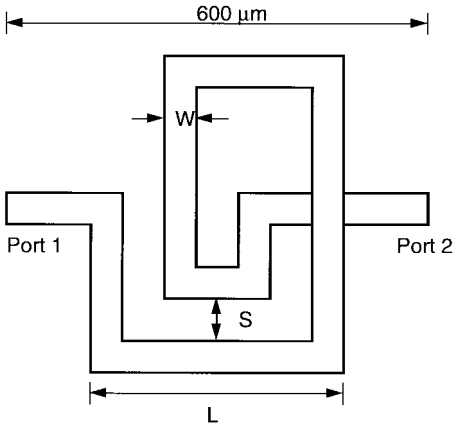

Fig. 3. Example layout of square spiral inductor with 1.5 turns. The other factors used in the experimental design are depicted as L, S, W which are length, spacing, and width, respectively.

The data set generated for this experimental design was selected to represent a range of inductance normally realized in MMIC applications. Also, some of the inductors went through resonance within the frequency range studied. The factors used in the experiment were the spiral inductor design parameters: width (W), spacing (S), length (L), and number of turns (T). These design factors, which are physically-based, are representative of the parameters that can be easily varied by a circuit designer when laying out a MMIC. While other parameters may be significant, those parameters are not directly controllable by the circuit designer. For example, substrate thickness is a significant parameter in microstrip design. However, the substrate thickness is usually constant for a given technological fabrication process.

The physical layout of the inductors used in the experiments is illustrated in Fig. 3. The inductors consisted of a square spiral without mitered corners. While W, S, L, and T were varied for each experiment, the linear separation between Port 1 and Port 2 was fixed at 600 μm. Air bridges were used to connect Port 2 to the center of the inductor structure. The fixed port separation was used to be compatible with a set of fabricated inductors, which required the fixed port separation to permit automated on-wafer probing.

The responses in the DoE were limited to a subset of the inductor's s-parameters for ease of experimentation. Since the inductors were reciprocal, s_{21} and s_{12} should be equal. Also, since the inductors used in this paper were nearly lossless, the magnitudes of s_{11} and s_{22} should be approximately equal to conserve energy. Therefore, the responses used in the DoE consisted of the magnitude and angle of s_{11}, the magnitude and angle of s_{21}, and the angle of s_{22} at a specified frequency.

This DoE yielded a MLPNN which is depicted in a block diagram in Fig. 4. The input parameters of the model are the frequency and the inductor's physical dimensions. The output is the set of computed s-parameters for the respective inductor at the specified frequency point.

A minimum of a three-level DoE was required since an inductor's s-parameters are typically nonlinear functions of the layout. For example, the angle of s_{22} at 7 GHz as a function of line spacing is depicted in Fig. 5. The width, length, and number of turns were held constant at 25, 300 μm, and 1.5,

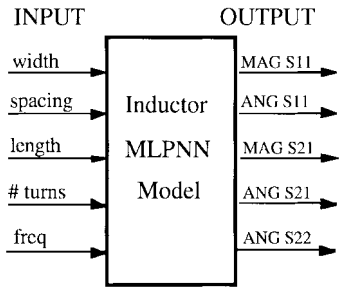

Fig. 4. Block diagram of MLPNN model. A separate MLPNN model was independently developed for each example.

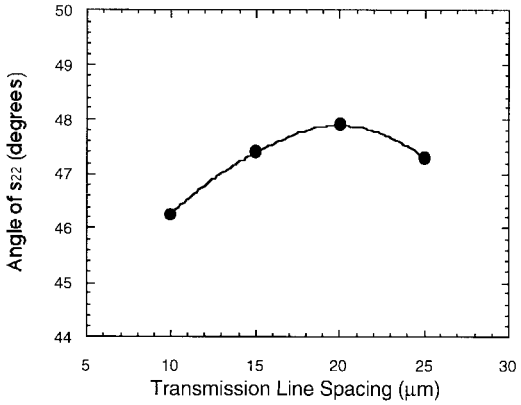

Fig. 5. Illustrative example of the nonlinear behavior of a square spiral inductor at 7 GHz. The width, length, and number of turns were 25 μ, 300 μm, and 1.5, respectively.

TABLE I
NOMINAL DESIGN VALUES USED IN FINAL DOE FOR TRAINING THE MLPNN

Factor	Level 1	Level 2	Level 3
Width (μm)	10	15	20
Spacing (μm)	10	20	25
Length (μm)	200	300	350
Number of Turns	1.5	2.5	3.5

respectively, while the spacing was varied over four levels. Only three levels were used in the final DoE to minimize the number of EM simulations required to generate the data set. However, four levels were used for each design factor in preliminary simulations to screen the parameter values to be used in the final three level DoE. The three values were selected such that a first-order fit could be made to the response locus. From the results depicted in Fig. 5, spacing values of 10, 20, and 25 μm were selected. The values of each design factor used in the final three-level DoE are given in Table I.

The potential levels of the design factors were constrained further. To ensure that the factors were orthogonal, the geometrical layout of the inductor was not minimized. Hence, those levels which would have made any parameter dependent upon another were excluded from the DoE. For example, referring to Fig. 3, a 1.5-turn inductor with a line width of 20 μm and a line spacing of 25 μm must have a length of at least 155 μm to be physically realizable. Also, a minimal layout would have required a length equal to 155 μm. For this example, any length less than or equal to 155 μm would be excluded from the DoE. Hence, any combination of factor levels which would have yielded a nonorthogonal or nonphysical combination was excluded from the desired full factorial DoE producing a fractional factorial DoE. This resulted in only 70 inductors being simulated to generate the data set as opposed to 81 in a full factorial DoE.

Sonnet's *em* [15], a commercially available EM simulator, was used to perform the EM simulations to generate the corresponding s-parameters for each inductor. The material parameters (such as resistivity and permittivity) used in the EM simulations were consistent with results obtained from inductors which were actually fabricated and characterized. The simulations were used to generate a table of s-parameters from 4 to 12 GHz in 1-GHz intervals for each inductor in the DoE. This set of s-parameters constituted the training set used to develop the MLPNN inductor model.

Additional EM simulations were completed to generate the test data used to characterize the MLPNNO's ability to generalize. The most significant benefit of this approach will be realized with the neural network's ability to predict the s-parameters for inductors with parameter values not included in the training set. A comprehensive test set was created to demonstrate the MLPNN inductor model's generalization capabilities. The test inductors were designed to exhibit several different variations of W, S, and L, with values not included in the training set. However, the test inductors used the same number of turns as were used with the training inductors (i.e., 1.5, 2.5, and 3.5) to simplify laying out the inductors and to limit the number of time-consuming EM simulations required to generate the test set.

More comprehensive training and test data could have been generated using a DoE with more than the minimal three levels to better capture the inductor's nonlinear response. However, for purposes of this paper, the use of only three levels was a compromise among accuracy, precision, and the time required to complete the EM simulations.

IV. EXPERIMENTS

Three separate experiments were conducted to demonstrate the feasibility of using the MLPNN approach to accurately model the scattering parameters of the MMIC spiral inductor. The first experiment was to create a C-band MLPNN model for the frequency range of 4–8 GHz. The second experiment was to create an X-band MLPNN model covering the frequency range of 8–12 GHz. In the third experiment a combined C–X-band MLPNN model was developed to cover the broader frequency range of 4–12 GHz. In each experiment the MLPNN had one hidden layer. The size of the hidden layer was determined experimentally by selecting the number of hidden nodes which resulted in the lowest training error, while maintaining adequate generalization. Each model took less than 15 min to train on a 125-MHz HP 9000/770 workstation.

The training set used for model development consisted of the 70 inductors from the initial DoE. This resulted in 350 training vectors for the C-band and X-band models and 630 for the combined C–X-band model. The difference in the

TABLE II
TEST INDUCTOR DESIGN PARAMETERS VALUES

Parameter	Notation	Value
Width (μm)	W	***5***,12,18,***25***
Spacing (μm)	S	***5***,***8***,15,18,22,***30***
Length (μm)	L	***150***,225,250,275,280,325,***375***

TABLE III
DISTRIBUTION OF TEST INDUCTORS PARAMETER DEVIATIONS

Parameter(s) in training set	Parameter(s) not in training set	Number of inductors with particular deviation
S,L	W	4
W,L	S	4
W,S	L	6
L	W,S	6
S	W,L	6
W	S,L	6
NONE	W,S,L	6

number of training vectors is due to the number of frequency points modeled.

Table II lists the design parameters and their values which were used in generating the test set. The values in bold italics were exclusive to the DoE range of each parameter. The remaining values were all inclusive to the DoE ranges. The concepts of exclusive and inclusive test vectors are analogous to extrapolated and interpolated values, respectively, in traditional regression analysis. Additionally, the distribution of the number of turns for the test inductors was eight with 1.5 turns, 22 with 2.5 turns, and eight with 3.5 turns.

The parameter values listed in Table II were combined in such a way that the test set consisted of inductors with one, two, or three parameters with values not included in the training set. Table III lists the distribution of these variations. The table lists which parameter values were in the training set, which were not, and the number of inductors in the test set which had that particular deviation from the training set. This test set design required the generation of an additional 38 inductors. EM simulations were performed on these test inductors, and the specific test vectors were formed in the same manner used in the DoE of the training inductors.

V. RESULTS

Upon completion of training, the models developed were tested and evaluated. This included the evaluation of the network's ability to learn the mappings of the training data, as well as its ability to generalize on the test set data. Each test vector is used as input to the respective MLPNN. The computed outputs represent the modeled s-parameters at the input frequency for each test inductor. For each individual output the modeled values were compared to the EM simulated values by computing the rmse as given in (4).

Also, to further quantify the MLPNN's modeling accuracy, the Pearson Product–Moment correlation coefficient (r), given in [16] as

$$r = \frac{\sum (x_i - \overline{x})(y_i - \overline{y})}{\sqrt{\sum (x_i - \overline{x})^2 \sum (y_i - \overline{y})^2}} \tag{5}$$

was calculated for each output. Where x_i is the EM simulated value, y_i is the MLPNN computed value, $\overline{x}$ is the EM-simulated sample mean, and $\overline{y}$ is the MLPNN computed sample mean.

TABLE IV
CORRELATION COEFFICIENT BETWEEN THE EM-SIMULATED AND MLPNN-COMPUTED OUTPUTS FOR THE C–X-BAND TRAINING SET

OUTPUT	MAG s_{11}	ANG s_{11}	MAG s_{21}	ANG s_{21}	ANG s_{22}
r	.9986	.9993	.9981	.9995	.9996
rmse	.0004001	.03681	.0003656	.03144	.02514

The correlation coefficient indicates how well the modeled values match the simulated values. A correlation coefficient near one indicates excellent predictive ability, while a coefficient near zero indicates little predictive ability. Scatter plots of the MLPNN-computed values versus the EM-simulated values are created to visually illustrate the modeling accuracy. Perfect accuracy would result in the data points forming a straight line along the diagonal axis.

The results of the C-band and X-band experiments were very good with correlations between the MLPNN-computed and EM-simulated values of greater than 0.98 for all modeled parameters. However, due to space limitations, only the results from the C–X-band experiment are presented.

A. C–X-Band MLPNN Model

The performance of the C-band and X-band MLPNN models were so promising and performed in such a similar manner that it was decided to conduct a third experiment. For this experiment, a single MLPNN inductor model was developed to predict the s-parameter responses over the broader 4–12-GHz frequency range.

1) Training Results: A single MLPNN, which had a hidden layer consisting of 32 neurons, was trained using 630 training vectors. The training set was a combination of the training sets from examples one and two. It contained the frequency and inductor s-parameter responses relative to the 4–12-GHz range. The correlation coefficient and rmse value for each output parameter, taken across all training vectors, is given in Table IV. The MLPNN computed outputs are very accurate with near perfect correlation coefficients of one. Fig. 6(a)–(d) shows scatter plots of EM-simulated and MLPNN-computed values for magnitude (MAG) s_{11}, angle (ANG) s_{11}, MAG s_{21}, and ANG s_{21}, respectively. These results are a further indication of the MLPNN's capability to capture the complex nonlinear inductor responses.

The accuracy of the C–X-band model was expected to decrease due to the complexity of example three. However, as can be seen from these illustrations and the associated r and rmse values, the accuracy remained nearly constant and actually increased for some parameters. This prediction accuracy may be attributed to the expanded data set, in the form of additional frequency points, available to the MLPNN during training. Training data is particularly important at the minimum and maximum frequency point. It was observed in examples one and two that the errors associated with the minimum and maximum frequency points (i.e., 4 and 8, 8 and 12, for examples one and two, respectively) were slightly greater than those for the intermediate frequency points. In the C-band and X-band models, 8 GHz was either a minimum or maximum frequency; however, in the combined training model

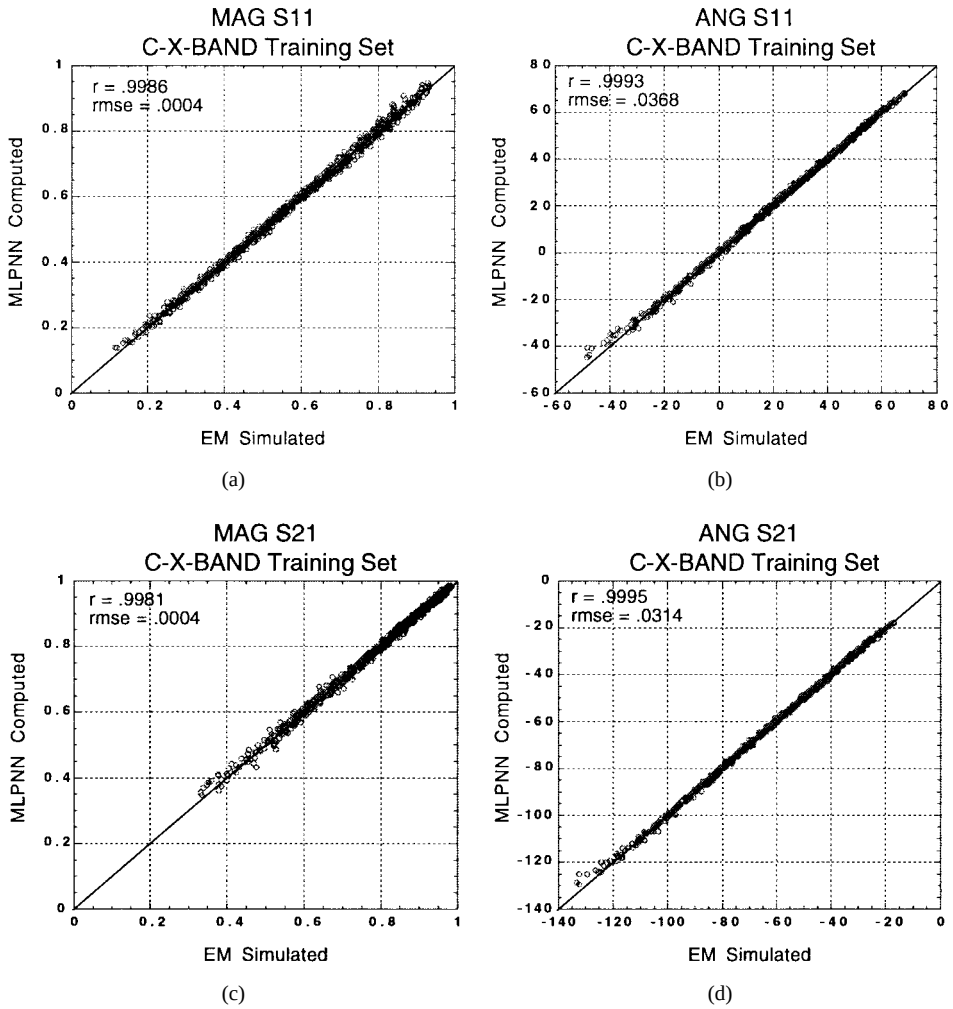

Fig. 6. Scatter plots of the EM-simulated and MLPNN-computed s-parameters for the C–X-band training set. (a) MAG s_{11}. (b) ANG s_{11}. (c) MAG s_{21}. (d) ANG s_{21}.

TABLE V
CORRELATION COEFFICIENT BETWEEN THE EM-SIMULATED AND MLPNN-COMPUTED OUTPUTS FOR THE C–X-BAND TEST SET

OUTPUT	MAG s_{11}	ANG s_{11}	MAG s_{21}	ANG s_{21}	ANG s_{22}
r	.9873	.9872	.9896	.9876	.9892
rmse	.001516	.1907	.001077	.1848	.1603

the additional information about the inductor's response on either side of 8 GHz was available. This resulted in increased model performance at 8 GHz.

2) Test Results: The combined test set for the C–X-band consisted of 342 vectors. The correlation coefficients and rmse values between the EM-simulated and MLPNN-output responses are given in Table V. Fig. 7(a)–(d) shows scatter plots of EM-simulated and MLPNN-computed values from the test set for the MAG s_{11}, ANG s_{11}, MAG s_{21}, and ANG s_{21}, respectively. The MLPNN computed responses for the test set also resulted in high correlations.

Comparing the scatter plots of Figs. 6 and 7, the grouping of test data points about the diagonal axis, while very tight, is not as tight as that for the training data. However, further analysis revealed that the largest errors where associated with inductors whose design parameters where exclusive to the DoE ranges. The rmse values in Table V are greatly affected by the exclusive test vectors. This is illustrated in Fig. 8(a) and (b). These figures show the squared error for each sample in the C–X-band test file for the output parameters, MAG s_{21} and ANG s_{21}, respectively. The largest errors are associated with inductors which had physical design parameters outside the DoE ranges. These results indicate that the MLPNN does not predict the s-parameters of inductors with design parameter values outside the ranges of the DoE as accurately as for those whose design parameters are inclusive to the DoE ranges. The same trends were observed for the C-band and X-band modeling results.

VI. DISCUSSION

The performance of the MLPNN varied with different training and test data. The results indicate that one can have high confidence in the MLPNN's predictive capability for design parameters and frequency points inclusive to the DoE ranges. This is particularly true for values which are at or very near the exact values used in the DoE, as illustrated by the training set scatter plots. However, the performance degraded for exclusive data sets. These results suggest that during the

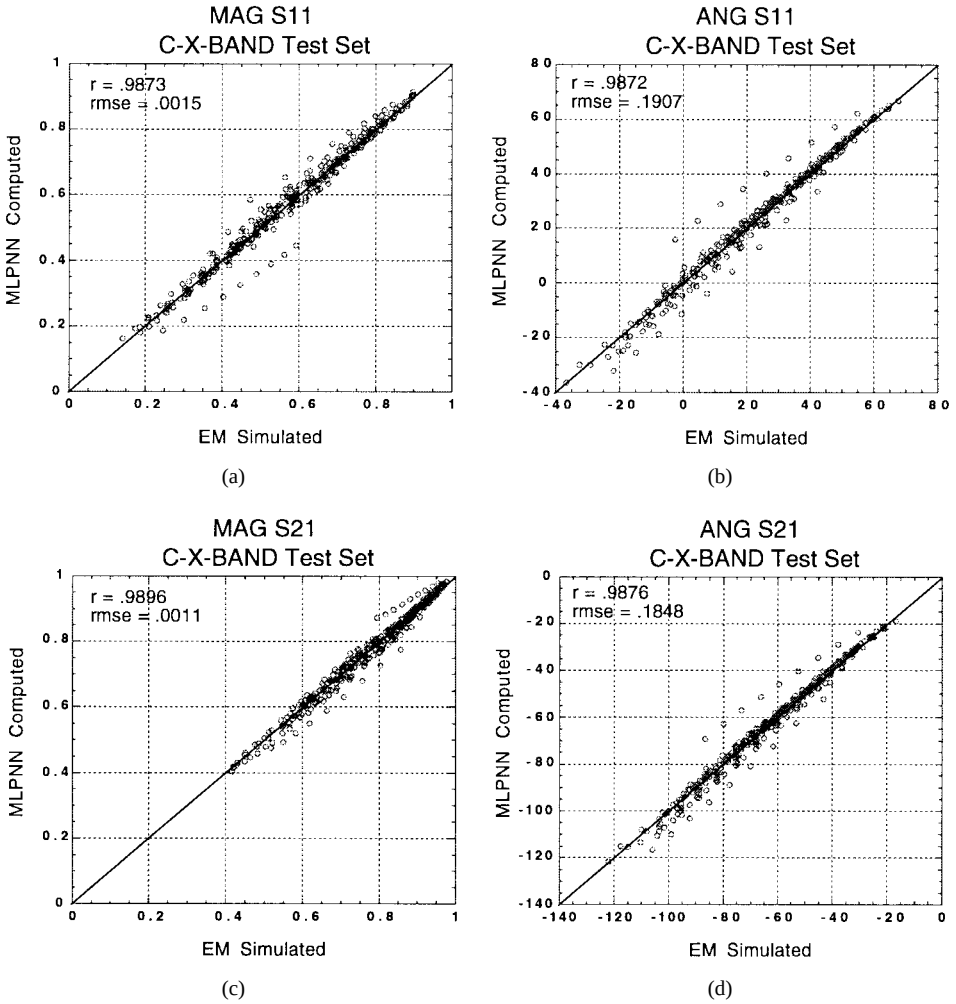

Fig. 7. Scatter plots of the EM-simulated and MLPNN-computed s-parameters for the C–X-band test set. (a) MAG s_{11}. (b) ANG s_{11}. (c) MAG s_{21}. (d) ANG s_{21}.

design of a DoE to generate an MLPNN training set, the factor levels should extend beyond the intended range of use. There does not appear to be a degradation of MLPNN performance for extended ranges, as revealed by the increased performance of the combined C–X-band MLPNN.

The C–X-band MLPNN model was implemented as a user-defined element into a popular circuit simulator. This enabled the MLPNN model to be used in the design, analysis, and optimization of microwave circuits. EM simulations are usually too time consuming to interactively perform these functions. The execution time for a full-wave EM simulation depends on the number of grid points used when meshing the structure and the numerical tolerances. The number of grid points greatly depends on the smallest critical geometric feature. For example, the time required for the EM simulation of a 2.5-turn spiral inductor on a 5-μm grid is about 3 min per frequency point. However, the time required for a similar inductor on a 2-μm grid is about 53 min per frequency point. These simulation times clearly limit the practicality of EM simulation in an interactive CAD environment.

The extensive computational effort required to generate the data used to train and test the MLPNN should not be underestimated. This effort may only be practical for smaller commonly used structures. The parameter coverage of the structures need to be properly envisaged up front.

The neural network approach used in this paper provides an approach for avoiding these long simulation times when evaluating small changes in the layout geometry. Once the network is trained, the computation time of the modeled outputs is negligible and is orders of magnitude faster than any single full-wave EM simulation.

VII. Conclusion

This paper presented an approach in which a neural network was employed to accurately model MMIC passive element characteristics. The MLPNN demonstrated the ability to compute s-parameters nearly as accurate as those obtained from full-wave EM simulations. It also has demonstrated the capability to generalize and to predict accurate model parameters for data outside the training set. Once trained, the computation time was negligible as compared to other techniques such as full-wave EM simulation. This computational speed makes the network suitable for interactive CAD applications. Also, this approach demonstrates that the perfor-

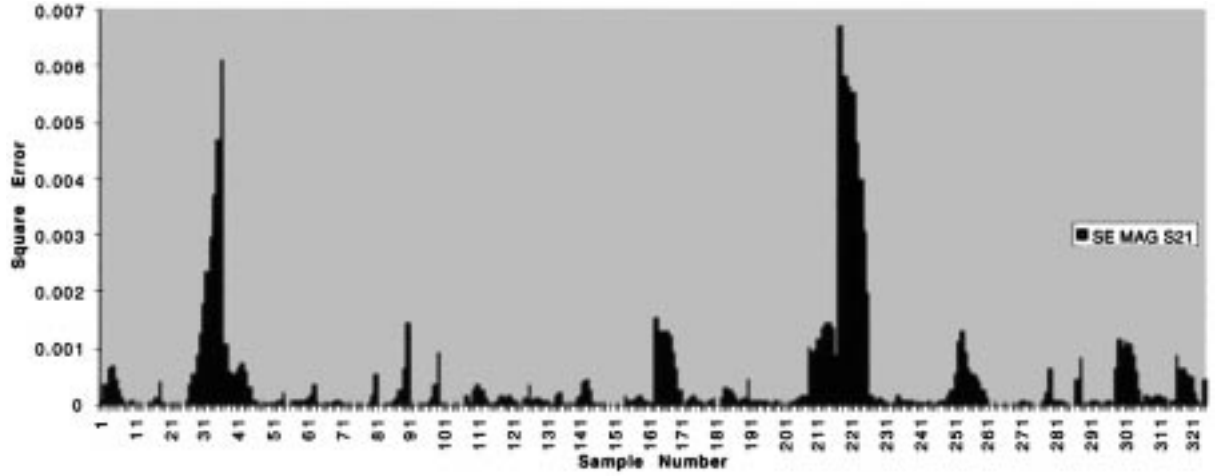

(a)

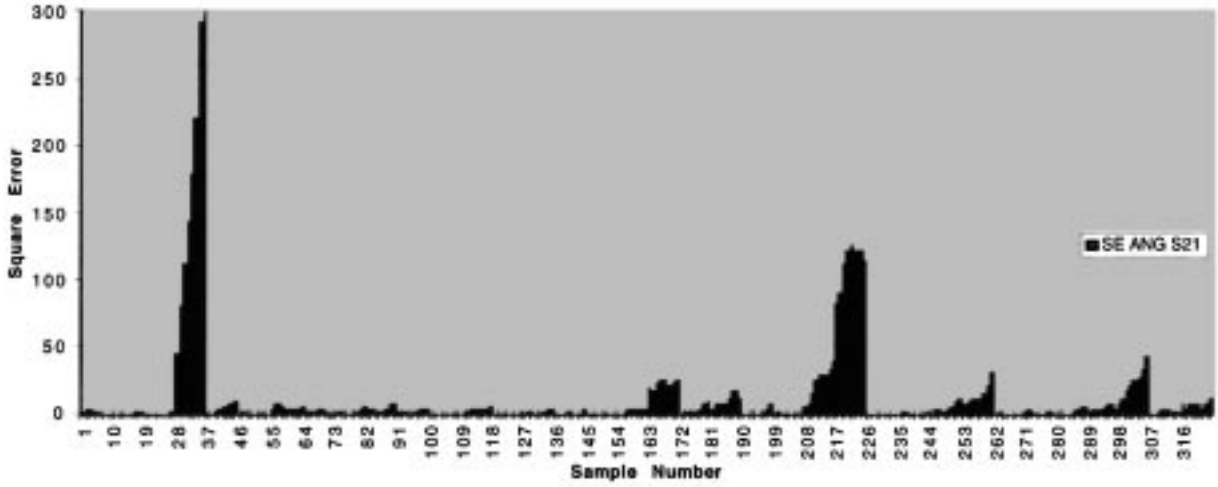

(b)

Fig. 8. Bar chart of the square error between simulated and MLPNN-computed s-parameters of each sample in the C–X-band test set. (a) MAG s_{21}. (b) ANG s_{21}.

mance of passive elements at microwave and/or millimeter-wave frequencies can be accurately predicted without the need to develop costly model libraries. Although the three examples illustrated only inductor passive-element modeling, the methodology may be extended, in principle, to other passive elements.

Recent literature has shown the emergence of complex BP training algorithms. In this training approach the error calculations and the resulting weight corrections are based on the difference between two complex vectors. Using a complex BP algorithm, the scalar errors are replaced with a true vector error and the trained response of magnitude and phase of a given s-parameter are more tightly coupled as a true vector quantity. Further research is currently underway to utilize these complex BP algorithms in the training of the MLPNN inductor models presented here.

ACKNOWLEDGMENT

The authors would like to thank the reviewers whose comments served to strengthen this manuscript.

REFERENCES

[1] M. Goldfarb and A. Platzker, "The effects of electromagnetic coupling on MMIC design," *Int. J. Microwave, mm-Wave CAE*, vol. 1, no. 1, pp. 38–47, 1991.

[2] S. Chaki, S. Aono, N. Andoh, Y. Sasaki, N. Tanino, and O. Ishihara, "Experimental study on spiral inductors," in *IEEE MTT-S Dig.*, vol. 2. Orlando, FL, June 1995, pp. 753–756.

[3] J. Rautio, "Reviewing available EM simulation tools," *Microwaves RF*, vol. 30, no. 6, pp. 7–10, June 1991.

[4] T. Horng and C. Wang, "Microstrip circuit design using neural networks," in *IEEE MTT-S Dig.*, vol. 1. Orlando, FL, May 1995, pp. 413–416.

[5] M. Smith, *Neural Networks for Statistical Modeling.* New York: Van Nostrand: 1993, pp. 117–129.

[6] D. Hush and B. Horne, "Progress in supervised neural networks," *Signal Process*, pp. 8–39, Jan. 1993.

[7] G. Cybenko, "Approximation by superpositions of a sigmoidal function," *Math. Cont., Sig., Sys.*, vol. 2, no. 4, pp. 303–314, Apr. 1989.

[8] A. Zaabab, Q. Zhang, and M. Nakhla, "Analysis and optimization of microwave circuits and devices using neural network models," in *IEEE MTT-S Dig.*, San Diego, CA, May 23–27, 1994, pp. 393–396.

[9] T. Horng, C. Wang, and N. Alexopoulos, "Microstrip circuit design using neural networks," in *IEEE MTT-S Dig.*, Atlanta, GA, June 14–18, 1993, pp. 413–415.

[10] P. Ojala, J. Saarinen, and K. Kaski, "Modified back-propagation neural network device characterization for VLSI circuit simulation," in *Proc. WCNN*, San Diego, CA, June 1994, pp. 413–415.
[11] G. Creech and J. Zurada, "GaAs MESFET dc characteristics and process modeling using neural networks," *Intel. Eng. Sys. Through Art. Neur. Net.* 1994, vol. 4, pp. 1005–1113.
[12] G. Creech, J. Zurada, and P. Aronhime, "Feedforward neural networks for estimating IC parametric yield and device characterization," in *Proc. IEEE Int. Symp. Circ. Sys.*, Seattle, WA, Apr. 30–May 3, 1995, vol. 2, pp. 1520–1523.
[13] J. M. Zurada, *Introduction to Artificial Neural Systems.* St. Paul, MN: West, 1992, pp. 186–190.
[14] J. Carroll and K. Chang, "Statistical computer-aided design for microwave circuits," *IEEE Trans. Microwave Theory Tech.*, vol. 44, p. 24–32, Jan. 1996.
[15] *em* Simulator, Ver. 2.4, Sonnet Software, Liverpool, NY, 1993.
[16] R. Scheaffer and J. McClave, *Statistics For Engineers.* Boston, MA: Duxbury Press, 1982, pp. 258–262.

Gregory L. Creech (S'93–M'95) received the B.S. and M.Eng. degrees in electrical engineering, both in 1988, and the Ph.D. degree in computer science and engineering, in 1996, from the University of Louisville, Louisville, KY.

He is a Project Engineer assigned to the Wright Laboratory's Avionics Directorate's Electron Devices Division, Wright-Patterson Air Force Base, Dayton, OH. He conducts in-house and contractual exploratory and advanced development programs, in the 0.1–300-GHz frequency range, to satisfy aerospace electronic performance and affordability needs. His current research interest include computational intelligence and adaptive distributed parallel computing techniques for the modeling and simulation of complex systems.

Bradley J. Paul received the B.S. degree in electrical engineering from Wright State University, Dayton, OH, and the M.S. degree in engineering management from the University of Dayton, Dayton, OH, in 1991 and 1995, respectively.

He is a Project Engineer assigned to the Wright Laboratory's Avionics Directorate's Electron Devices Division, Wright-Patterson Air Force Base, Dayton, OH. He conducts in-house and contractual exploratory and advanced development programs to develop, demonstrate, and transition robust, high-density packaging, and interconnect technologies for digital, microwave, and millimeter-wave military aerospace systems.

Christopher D. Lesniak received the B.S. degree in electrical engineering from the Lawrence Technological University, Southfield, MI, in 1988 and is currently pursuing a M.Eng. degree in engineering management at the University of Dayton, Dayton, OH.

He is a Project Engineer assigned to Wright Laboratory's Avionics Directorate's Electron Devices Division, Wright-Patterson Air Force Base, Dayton, OH. He conducts in-house and contractual exploratory and advanced development programs in the microwave and millimeter-wave frequency ranges.

Thomas J. Jenkins (S'82–M'84) received the B.S.E.E. degree from the University of South Florida, Tampa, FL, and the M.S.E.E. degree from the Air Force Institute of Technology, Wright-Patterson AFB, Dayton, OH, in 1984 and 1989, respectively.

In 1995, he joined the Northeast Consortium for Engineering Education at Port Royal, VA, as a Research Scholar, after retiring that year from the United States Air Force. He is currently a Research Scientist with the Wright State University Research Center, Dayton, OH. He is investigating novel microwave devices and design techniques at Wright Laboratory, Wright-Patterson Air Force Base, Dayton, OH.

Mr. Jenkins is a member of Tau Beta Pi, Eta Kappa Nu, and Phi Kappa Phi.

Mark C. Calcatera (M'88) was born in Detroit, MI, in 1949. He received the B.S. degree from the University of Detroit, Detroit, MI, and the M.S. degree, both in electrical engineering, from Ohio State University, Columbus, in 1972 and 1978, respectively, and attended post-graduate training at the University of Michigan, Ann Arbor, MI, from 1980 to 1981.

Since 1984, he has served as the Chief of the Microwave Components Branch, at Wright Laboratory. He has authored several technical papers and has been granted three U.S. patents with two others pending. His interests span all aspects of military specific and dual-use RF component technology, with special emphasis on the nonlinear modeling of solid state power devices and circuits.

Mr. Calcatera presently serves on the technical program committees for MTT-S International Microwave Symposium (IMS) as well as the Microwave and Millimeter-Wave Circuits Symposium.